Sensors and Materials, Vol. 30, No. 4 (2018) 925–932
MYU Tokyo

S & M 1550

Analyses of Responsivity and Quantum Efficiency of p-Si/i-β-$FeSi_2$/n-Si Photodiodes

Jung-Sheng Huang,[1] Kuan-Wei Lee,[1*] Cheng-Yao Huang,[1] and Shih-Feng Wang[2]

[1]Department of Electronic Engineering, I-Shou University
No.1, Sec. 1, Syuecheng Rd., Dashu District, Kaohsiung City 84001, Taiwan, R.O.C.
[2]Department of Aviation & Communication Electronics, Air Force Institute of Technology,
Kaohsiung, 820 Taiwan, R.O.C.

(Received November 1, 2017; accepted April 13, 2018)

Keywords: p-Si/i-β-$FeSi_2$/n-Si photodiode, responsivity, quantum efficiency

In this study the responsivity and quantum efficiency of p-Si/i-β-$FeSi_2$/n-Si double-heterostructure photodiodes and p-Si/i-Si/n-Si photodiodes are investigated by self-developed analytical methods. The dark current densities of both β-$FeSi_2$ and Si p–i–n photodiodes under the reverse bias condition are calculated by solving the diffusion current densities of minority carriers. The photocurrent densities of both p–i–n photodiodes under illumination with reverse bias are mainly calculated by solving the drift current densities in the depletion regions. When the β-$FeSi_2$ p–i–n photodiode incident wavelength, λ, is less than 0.6 μm, the magnitudes of responsivity and quantum efficiency are almost zero for different intrinsic thicknesses. The maximum responsivity, R = 0.65 A/W, and quantum efficiency, η = 65%, are both at λ = 1.2 μm and the intrinsic β-$FeSi_2$ layer thickness is 100 μm. The calculated responsivity of the Si p–i–n photodiode is consistent with the reported studies. Therefore, the analysis methods and results are valid in this work. These results indicate the high applicability of β-$FeSi_2$ to near-infrared photodiodes integrated with Si. Therefore, the p-Si/i-β-$FeSi_2$/n-Si photodiode is a new high-efficiency light sensor device applicable to optical fiber communications.

1. Introduction

A silicide is a compound that has silicon with larger electropositive elements. Metal silicides have been widely investigated for several years because of their potential applications in electronics.[1] Semiconducting beta-phase iron disilicide (β-$FeSi_2$) is a metal silicide and is a very promising Si-based new material for optoelectronic applications.[2–4] β-$FeSi_2$ has a large optical absorption coefficient ($\alpha > 10^5$ cm^{-1} at 1.5 eV) and a direct band gap of 0.85–0.87 eV.[5–7] β-$FeSi_2$ thin films can be epitaxially grown on Si substrates with small lattice mismatches of 2–5%.[8] β-$FeSi_2$ is currently attracting considerable attention as a material for light-emitting diodes.[9] Huang *et al.*[10] reported a conversion efficiency of 27.8% for a n-Si/i-β-$FeSi_2$/p-Si double-heterostructure solar cell. Light detection in the near-infrared region, especially at the 1.3 and 1.55 μm wavelengths, is a significant topic for optical fiber communication systems.

*Corresponding author: e-mail: kwlee@isu.edu.tw
http://dx.doi.org/10.18494/SAM.2018.1795

ISSN 0914-4935

Light sources and detectors that are compatible with conventional Si technology are needed for future integrated optoelectronics.[11] Izumi *et al.*[12] reported a near-infrared photodetection of β-$FeSi_2$ /Si heterojunction photodiodes with a responsivity of 16.6 mA/W.

Therefore, in this study, the responsivity and quantum efficiency of p-Si/i-β-$FeSi_2$/n-Si double-heterostructure photodiodes are investigated by self-developed analytical methods. For photodiodes, the p–i–n structure usually has superior responsivity to that of the p–n structure. Since a built-in electric field exists in the intrinsic layer, the generated electron–hole pairs in the intrinsic layer drift owing to the electric field and produce a large photocurrent and responsivity. In addition, the intrinsic silicide layer does not need doping and its manufacturing process is compatible with that of well-established Si photodiodes. The generation rates of electron–hole pairs in the β-$FeSi_2$ p–i–n photodiode are calculated first. Then the photocurrent density under illumination with reverse bias is mainly calculated by integrating the generation rates of electron–hole pairs over the whole depletion region. The dark current density of the β-$FeSi_2$ p–i–n photodiode under the reverse bias condition is calculated by solving the diffusion current densities of minority carriers. The responsivity of the photodiode is the photocurrent divided by the incident light power, and the quantum efficiency of the photodiode can be obtained from the responsivity.

The calculated maximum responsivity of the β-$FeSi_2$ p–i–n photodiode, R = 0.65 A/W, and quantum efficiency, η = 65%, are both at λ = 1.2 μm, and the intrinsic β-$FeSi_2$ layer thickness is 100 μm. The responsivity and quantum efficiency of p-Si/i-Si/n-Si photodiodes are also calculated for comparison. The calculated maximum responsivity of the Si p–i–n photodiode is R = 0.55 A/V at λ = 0.9 μm, which is consistent with the reported measurement results.[13] Thus, the calculation results in this work are valid. These results indicate the high application potential of β-$FeSi_2$ as near-infrared photodiodes integrated with Si. Therefore, the p-Si/i-β-$FeSi_2$/n-Si photodiode is a new high-efficiency light sensor device applicable to optical fiber communications.

2. Analysis Methods

The p–i–n photodiode device structure under investigation is shown in Fig. 1. The p–i–n photodiode is under reverse bias and the light is incident in the x-direction. At the surface of the photodiode (i.e., at x = 0 in Fig. 1), the generation rate of electron–hole pairs, $G_0(\lambda)$ ($m^{-3}s^{-1}$), is

$$G_0(\lambda) = \eta_i [1 - R(\lambda)] \frac{I_{opt}}{\hbar\omega} \alpha(\lambda), \tag{1}$$

λ = wavelength of incident light (m),
η_i = intrinsic quantum efficiency accounting for the average number (100% maximum) of electron–hole pairs generated per incident photon,
$R(\lambda)$ = optical reflectivity between air and the semiconductor,
I_{opt} = incident optical power intensity (Wm^{-2}),
$\hbar\omega$ = energy of the incident photon (J),
$\alpha(\lambda)$ = absorption spectrum (m^{-1}).

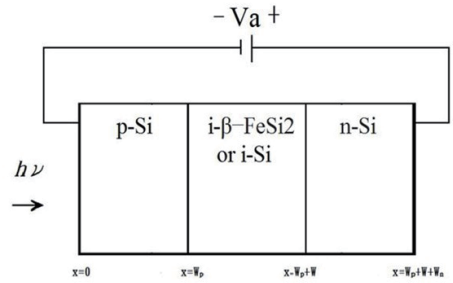

Fig. 1. The p-Si/i-β-$FeSi_2$/n-Si double-heterostructure photodiode.

The absorption spectra of β-$FeSi_2$ and Si are obtained using the experiment results reported in Refs. 5 and 13. The generation rate of the electron–hole pairs in the photodiode device ($x > 0$) is given as

$$G(x, \lambda) = G_0(\lambda) e^{-\partial(\lambda)x}. \tag{2}$$

The dark current density of the β-$FeSi_2$ p–i–n photodiode under the reverse-bias condition is calculated as

$$\begin{aligned} J_{dark} &= J_{n,diff}|_{x=Wp-Xp} + J_{p\cdot diff}|_{x=Wp+W+Xn} \\ &= qD_n \frac{dn_p}{dx}|_{x=Wp-Xp} - qD_p \frac{dp_n}{dx}|_{x=Wp+W+Xn}, \end{aligned} \tag{3}$$

where X_p and X_n are the depletion region thicknesses of p-Si and n-Si, respectively, and W is the intrinsic layer thickness, $J_{n,diff}|_{x=Wp-Xp} = qD_n \frac{dn_p}{dx}|_{x=Wp-Xp}$ is the free electron diffusion current density at the edge of the p-Si depletion region, and $J_{p,diff}|_{x=Wp+W+Xn} = -qD_p \frac{dp_n}{dx}|_{x=Wp+W+Xn}$ is the hole diffusion current density at the edge of the n-Si depletion region. Thus, the dark current density of the p–i–n photodiode is the sum of the minority carrier diffusion current densities.

With illumination under the reverse-bias condition, the drift current density due to optical generation in the depletion regions is calculated as

$$\begin{aligned} J_{drift} &= q \int_{X_p} G_0\,(\mathrm{Si})\, e^{-\alpha(\mathrm{Si})x} dx \\ &+ q \int_{i-layer} G_0\,(\beta\text{-}FeSi_2)\, e^{-\alpha(\beta\text{-}FeSi_2 \text{ or Si})x} dx \\ &+ q \int_{X_n} G_0\,(\mathrm{Si})\, e^{-\alpha(\mathrm{Si})x} dx, \end{aligned} \tag{4}$$

where the first term accounts for the drift current density obtained from the depletion region of

p-Si, the second term is the drift current density of the intrinsic β-$FeSi_2$ layer, and the third term is the drift current density of the depletion region of n-Si.

The total photocurrent density J_{ph} is given by

$$J_{ph} = J_{n.diff} + J_{p.diff} + J_{drift}. \tag{5}$$

The responsivity R of a photodiode characterizes its performance in terms of the photocurrent generated ($I_{ph} = J_{ph} A$) per incident optical power ($P_o = I_o A$) at a given wavelength.

$$R = \frac{I_{ph}}{P_o} = \frac{J_{ph}}{I_o} \tag{6}$$

The quantum efficiency η is calculated as

$$\eta = \frac{\frac{I_{ph}}{e}}{\frac{P_o}{\hbar\omega}} = R\frac{\hbar\omega}{e}, \tag{7}$$

where $e = 1.6 \times 10^{-19}$ C.

3. Discussion

By solving Poisson's equation, the calculated equilibrium energy band diagram of the p-Si/i-β-$FeSi_2$/n-Si photodiode is shown in Fig. 2. The thicknesses of the p-Si and n-Si layers are both 500 nm. The β-$FeSi_2$ layer is intrinsic and the thickness is between 1 and 100 μm. The doping concentrations of p-Si and n-Si layers are both 10^{17} cm^{-3}. The calculated dark current densities of β-$FeSi_2$ and Si p–i–n photodiodes as a function of the reverse bias voltages V_a are shown in Fig. 3. The dark current densities increase with increasing reverse bias voltage. The

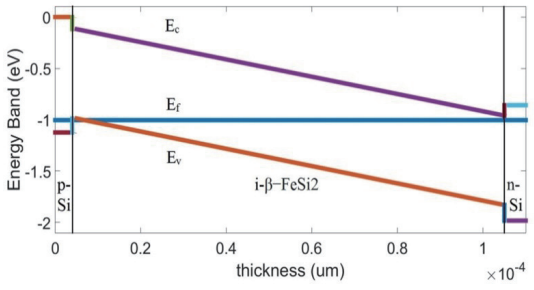

Fig. 2. (Color online) Calculated equilibrium energy band diagram of β-$FeSi_2$ p–i–n photodiode.

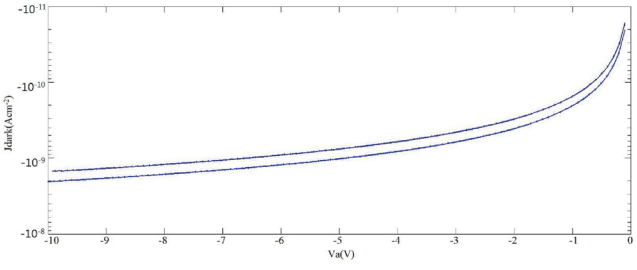

Fig. 3. (Color online) Calculated dark current density as a function of reverse bias voltage V_a. The upper curve is the dark current density of the Si photodiode. The lower curve is the dark current density of the β-$FeSi_2$ photodiode.

magnitude of the dark current densities is larger for the β-$FeSi_2$ p–i–n photodiode than for the Si p–i–n photodiode. The calculated electron–hole generation rates $G(x, \lambda)$ as a function of the position x for the β-$FeSi_2$ p–i–n photodiode with different incident wavelengths λ are shown in Fig. 4. At the incident wavelength λ of 0.3 μm, the absorption coefficient of β-$FeSi_2$ is very large, and the generation rate decreases exponentially with increasing distance x. At the incident wavelength λ of 1.1 μm, as the wavelength is increased, the absorption coefficient of β-$FeSi_2$ becomes smaller, and thus the slope of the generation rate decreases in the whole p–i–n diode. When the incident wavelength $\lambda > 1.14$ μm, the generation rate is very large and is almost constant. Now the energy of the incident photon is less than the energy gap of Si (Eg = 1.12 eV, corresponding to $\lambda = 1.1$ μm), therefore, the generation rate is zero in the p-Si and n-Si regions. However, in the intrinsic β-$FeSi_2$ layer, the generation rate for $\lambda = 1.14$ μm is very large and almost constant. The calculated generation rates of the β-$FeSi_2$ p–i–n photodiode with the intrinsic layer thickness of 100 μm are shown in Fig. 5. The curves indicate that the generation rates are less than 10^{10} $cm^{-3}s^{-1}$ for all incident wavelengths when the intrinsic layer thickness is larger than 30 μm. Comparison of Fig. 4 with Fig. 5 shows that when the intrinsic layer thickness is increasing, the generated free electron and hole concentrations are also increased at the incident wavelength $\lambda = 1.1$ to 1.2 μm. Thus, the generated photocurrent densities J_{ph} are increased.

The calculated generation rates of the p-Si/i-Si/n-Si photodiode are shown in Fig. 6. The intrinsic Si layer thickness is 1 μm. At the incident wavelength $\lambda = 0.3$ μm, the absorption coefficients of Si are large, and the generation rates are decreased exponentially. When the incident wavelength λ is greater than 0.7 μm, the absorption coefficient of Si becomes smaller and the generation rates are almost constant. The maximum generation in the intrinsic Si layer is at $\lambda = 0.9$ μm.

Under illumination with the reverse-bias voltage V_a of −10 V, the calculated photocurrent densities of the β-$FeSi_2$ p–i–n photodiode as a function of the incident wavelengths are shown in Fig. 7. The intrinsic layer thickness is 1 μm. The photocurrent densities J_{ph} are negligible when the incident wavelength λ is less than 0.6 μm. The maximum value of J_{ph} is about 23

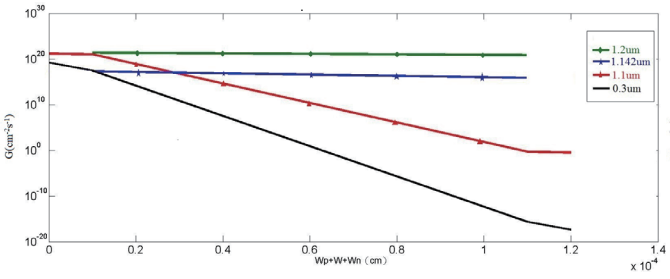

Fig. 4. (Color online) Calculated generation rate of electron–hole pairs for the β-$FeSi_2$ photodiode with different wavelengths as a function of position x. The intrinsic layer thickness is 1 μm.

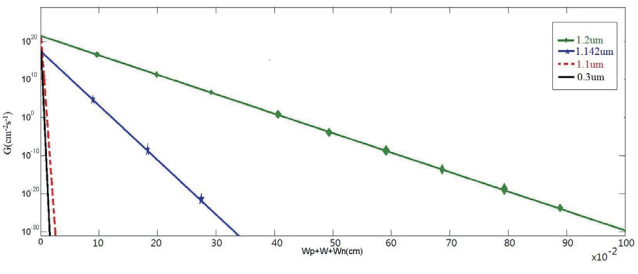

Fig. 5. (Color online) Calculated generation rate of electron–hole pairs for the β-$FeSi_2$ photodiode. The intrinsic layer thickness is 100 μm.

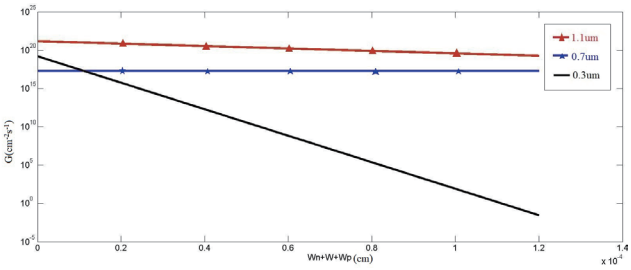

Fig. 6. (Color online) Calculated generation rate for the Si p–i–n photodiode. The intrinsic layer thickness is 1 μm.

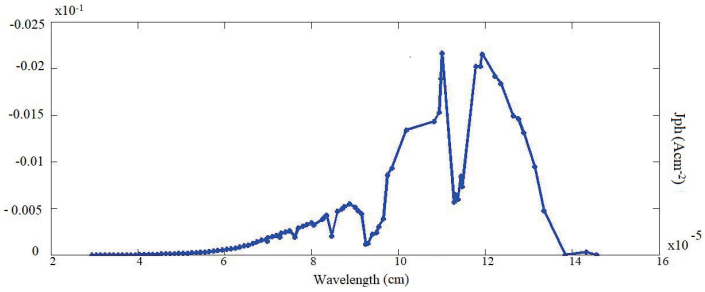

Fig. 7. (Color online) Calculated photocurrent densities of β-$FeSi_2$ p–i–n photodiode as a function of incident wavelength.

mA/cm^2 at both λ = 1.1 and 1.2 μm. The decrease in the magnitude of J_{ph} between λ = 1.1 and 1.2 μm is due to the generation rates being zero for Si at λ > 1.1 μm. The calculated photocurrent density of the β-$FeSi_2$ p–i–n photodiode with the intrinsic layer thickness of 100 μm is shown in Fig. 8. The maximum photocurrent density is about 33 mA/cm^2 at λ = 1.2 μm. The maximum photocurrent density increases with increasing intrinsic layer thickness from 1 to 100 μm. The calculated photocurrent densities of the Si p–i–n photodiode with the intrinsic layer thickness of 1 μm are shown in Fig. 9. At the incident wavelength λ of less than 0.3 μm, the photocurrent density is small. The maximum photocurrent density is about 11 mA/cm^2 at λ = 0.9 μm.

The calculated responsivities R of β-$FeSi_2$ p–i–n photodiodes as a function of the incident wavelength λ are shown in Figs. 10 and 11. The incident light power P_o is 1 mW. Therefore, the responsivity is proportional to the photocurrent density. The intrinsic layer thickness is 1 μm in Fig. 10 and 100 μm in Fig. 11. For the incident wavelength λ of less than 0.6 μm, the responsivity of β-$FeSi_2$ p–i–n photodiodes is negligible. For the incident wavelength λ greater than 1.1 μm, the responsivity increases as the intrinsic layer thickness increases. The maximum responsivity with the reverse-bias voltage V_a of −10 V is R = 0.65 A/W at λ = 1.2 μm with the intrinsic layer thickness of 100 μm. The calculated responsivities of the Si p–i–n photodiode are shown in Fig. 12. The intrinsic layer thickness is 1 μm. The maximum responsivity is shifted to longer incident wavelength as the intrinsic layer thickness increases. The maximum responsivity is 0.5 A/W at the incident wavelength λ of 0.9 μm with V_a of −10 V. The calculated responsivity of the Si p–i–n photodiode is consistent with the reported measured responsivity of the Si p–i–n photodiode.[13] Thus, the calculation results in this work are valid.

The calculated quantum efficiency of the β-$FeSi_2$ p–i–n photodiodes as a function of incident wavelength λ is shown in Fig. 13. The β-$FeSi_2$ intrinsic layer thickness is 1 μm. The quantum efficiency has the same characteristics as the responsivity. The maximum quantum efficiency of the β-$FeSi_2$ p–i–n photodiode is η = 75% at λ = 1.2 μm with the intrinsic layer thickness of 100 μm and the reverse-bias voltage V_a of −10 V. These results indicate the high applicability of β-$FeSi_2$ to near-infrared photodiodes integrated with Si. Therefore, the p-Si/i-β-$FeSi_2$/n-Si photodiode is a new high-efficiency light sensor device applicable to optical fiber communications.

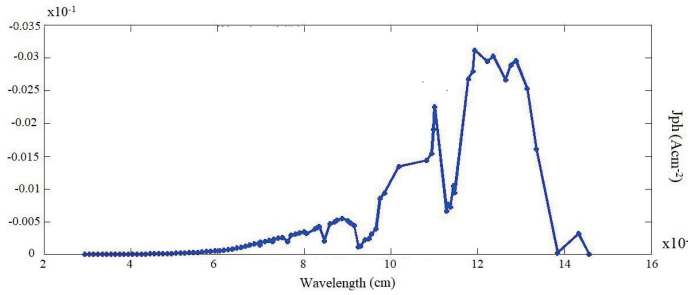

Fig. 8. (Color online) Calculated photocurrent densities of β-$FeSi_2$ p–i–n photodiode with the intrinsic layer thickness of 100 μm.

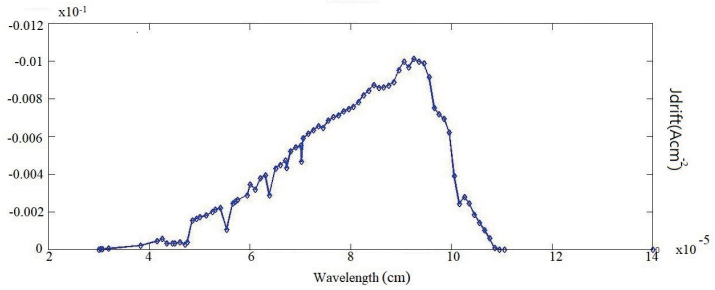

Fig. 9. (Color online) Calculated photocurrent densities of Si p–i–n photodiode with the intrinsic layer thickness of 1 μm.

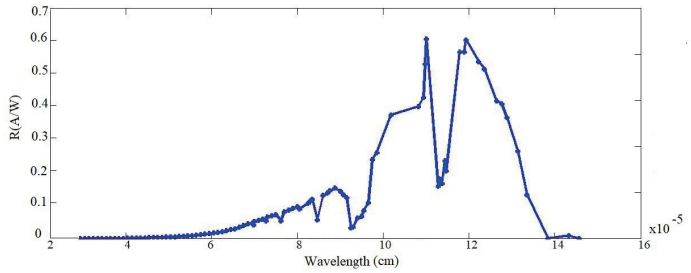

Fig. 10. (Color online) Calculated responsivity of β-$FeSi_2$ p–i–n photodiode as a function of incident wavelength λ. The intrinsic layer thickness is 1 μm.

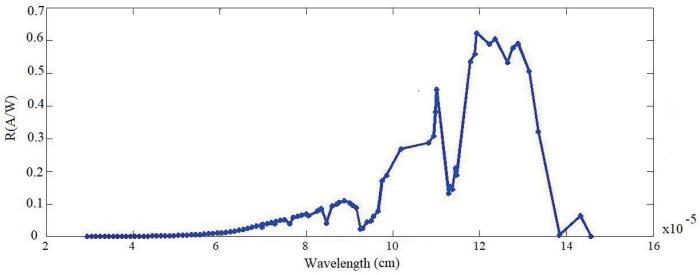

Fig. 11. (Color online) Calculated responsivity of β-$FeSi_2$ p–i–n photodiode as a function of the incident wavelength λ. The intrinsic β-$FeSi_2$ layer thickness is 100 μm.

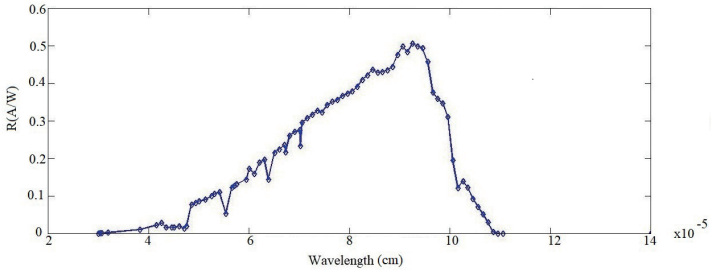

Fig. 12. (Color online) Calculated responsivity of Si p–i–n photodiode as a function of the incident wavelength λ. The intrinsic Si layer thickness is 1 μm.

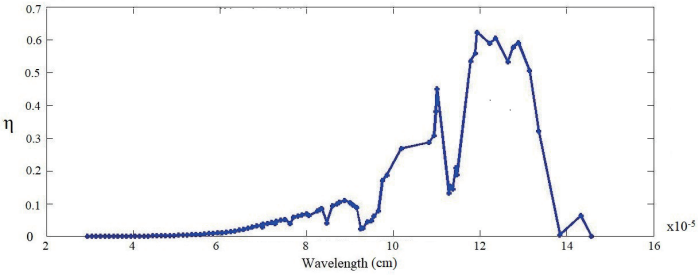

Fig. 13. (Color online) Calculated quantum efficiency of β-$FeSi_2$ p–i–n photodiode as a function of incident wavelength λ. The intrinsic β-$FeSi_2$ layer thickness is 100 μm under the reverse-bias voltage V_a of −10 V.

4. Conclusions

The responsivity and quantum efficiency of both p-Si/i-β-$FeSi_2$/n-Si and p-Si/i-Si/n-Si photodiodes were investigated by self-developed analytical methods. The dark current densities were calculated first, then the generation rates of electron–hole pairs under illumination. The photocurrent densities of the p–i–n photodiodes with illumination under the reverse-bias condition were calculated. Then, the responsivity and quantum efficiency could be obtained.

For the incident wavelength λ of less than 0.6 μm, the responsivity and quantum efficiency were negligible for β-$FeSi_2$ p–i–n photodiodes. For $\lambda > 1.1$ μm, the responsivity and quantum efficiency of β-$FeSi_2$ p–i–n photodiodes increased as the intrinsic layer thickness increased from 1 to 100 μm. The maximum responsivity was 0.65 A/W and the quantum efficiency was 75% for the β-$FeSi_2$ p–i–n photodiode at $\lambda = 1.2$ μm with the intrinsic layer thickness of 100 μm. The calculated maximum responsivity of the Si p–i–n photodiode was 0.5 A/W at $\lambda = 0.9$ μm with the intrinsic layer thickness of 1 μm and $V_a = -10$ V. These calculation results indicated the high applicability of β-$FeSi_2$ to near-infrared photodiodes integrated with Si and that the p-Si/i-β-$FeSi_2$/n-Si photodiode may be a new high-efficiency light sensor device applicable to optical fiber communications.

References

1 S. P. Murarka: J. Vac. Sci. Tech. **17** (1980) 775.
2 Y. Terai, T. Higashi, T. Hattori, K. Ogi, and S. Ikeda: Jpn. J. Appl. Phys. **56** (2017) 05DD03.
3 T. Taniguchi, S. Sakane, S. Aoki, R. Okuhata, T. Ishibe, K. Watanabe, T. Suzuki, T. Fujita, K. Sawano, and Y. Nakamura: J. Elec. Mater. **46** (2017) 3235.
4 A. Nozariasbmarz, P. Roy, Z. Zamanipour, J. H. Dycus, M. J. Cabral, J. M. LeBeau, J. S. Krasinski, and D. Vashaee: APL Mater. **4** (2016) 104814.
5 D. Leong, M. Harry, K. J. Reeson, and K. P. Homewood: Nature **387** (1997) 686.
6 K. Noda, Y. Terai, S. Hashimoto, K. Yoneda, and Y. Fujiwara: Appl. Phys. Lett. **94** (2009) 241907.
7 G. K. Dalapati, S. L. Liew, A. S. W. Wong, Y. Chai, S. Y. Chiam, and D. E. Chi: Appl. Phys. Lett. **98** (2011) 013507.
8 J. E. Mahan, V. Le Thanh, J. Chevrier, I. Berbezier, J. Derrien, and R. G. Long: J. Appl. Phys. **74** (1993) 1747.
9 M. Suzuno, S. Murase, T. Koizumi, and T. Suemasu: Appl. Phys. Express **1** (2008) 021403.
10 J. S. Huang, K. W. Lee, and Y. H. Tseng: J. Nanomater. **2014** (2014) 238291.
11 H. El Dirani, M. Casale, and S. Kerdiles: IEEE Techn. Lett. **30** (2018) 355.
12 S. Izumi, M. Shaban, N. Promros, K. Nomoto, and T. Yoshitake: Appl. Phys. Lett. **102** (2013) 032107.
13 S. O. Kasap: Optoelectronics and Photonics (Pearson, Edinburgh Gate, 2013) 2nd ed., p. 391.